Microwave response of anisotropic high-temperature-superconductor crystals

C. E. Gough and N. J. Exon
School of Physics and Space Research, Superconductivity Research Group, University of Birmingham, Birmingham B15 2TT, United Kingdom
(Received 25 January 1994)

Microwave penetration and losses are derived for the anisotropic normal and superconducting states of single crystals in the shape of thin platelets oriented parallel and perpendicular to the oscillating electromagnetic field. For platelet crystals with the microwave field parallel to the major flat faces, the large anisotropy in the normal state can result in dissipation dominated by microwave field penetration through the thin edges rather than across the main faces. The influence of the extreme anisotropy is also considered for the superconducting state and can account for an anomalous peak in microwave loss below T_c sometimes observed in Bi-Sr-Ca-Cu-O crystals. When crystals are mounted with their flat faces perpendicular to the microwave field, the losses in both the normal and superconducting states are shown to be strongly peaked towards the outer perimeter of the crystals. This makes critical demands on the degree of perfection of such regions, if the microwave measurements are not to be complicated by nonintrinsic effects associated with local imperfections.

I. INTRODUCTION

Measurements of the complex surface impedance, $Z_s = R_s + iX_s$, have been widely used to investigate fundamental superconducting properties of high-temperature superconductors (HTS).[1-11] Measurement of the reactive component $X_S(T) = \mu_0 \omega \lambda(T)$ provides a convenient method for determining $\lambda(T)$, the superconducting penetration depth. In contrast to the BCS and two-fluid model predictions, the penetration depth derived from microwave measurements on thin film HTS samples varies rather closely as $(1-t^2)^{-1/2}$,[4-6,11] where t is the reduced temperature T/T_c. However, in recent measurements on untwinned $YBa_2Cu_3O_{7-\delta}$ (YBCO) single-crystal platelets,[7] a linear temperature dependence was observed at low temperatures, providing possible evidence for d-state pairing and nodal lines of the superconducting energy gap on the Fermi surface.[4,9]

Once the penetration depth is known, microwave losses from thermally excited "normal" electrons can be derived by assuming a two-fluid model, which predicts a surface resistance $R_s = \frac{1}{2}\mu_0^2 \omega^2 \lambda^3 \sigma_n'(T)$, where $\sigma_n'(T)$ is the effective conductivity of the thermally excited quasiparticles. Of particular interest is an apparent increase in the quasiparticle mean free path deduced from microwave measurements on YBCO single crystals by Bonn *et al.*[10] These measurements are consistent with an apparent increase in the quasiparticle mean free path because of a reduced scattering from antiferromagnetic spin fluctuations resulting from a proposed gap in their spectrum, which opens up below T_c, as inferred from inelastic neutron scattering[12] and nuclear quadrupole resonance[13] measurements.

Microwave measurements thus provide important information about the nature of the superconducting ground state and the thermally excited quasiparticles. It is therefore important to be confident that microwave surface impedance measurements probe intrinsic properties and are not affected by unwanted experimental artifacts. In this paper we consider two potential problems that arise in microwave measurements on thin platelet crystals of highly anisotropic high-temperature superconductors. In particular, we show that the large anisotropy and high resistivity in the c direction can result in an anomalous peak in the microwave absorption in the superconducting state, for electromagnetic field parallel to the ab planes. If measurements are made with the typical platelet crystals perpendicular to the microwave field, the concentration of field near the edges leads to highly localized microwave losses in just those regions of the crystals that are most susceptible to damage, so that the measured microwave losses may not be intrinsic.

The two experimental configurations of interest for measurements on high-T_c (HTC) single crystals are illustrated in Figs. 1(a) and 1(b). In the first, the oscillating microwave field $h_{\mu\text{wave}}$ is parallel to the major flat surfaces of what is usually a rather thin platelet crystal. In this configuration the induced microwave currents flow across the major flat faces but also across the thin edge surfaces. For an isotropic material, the penetration and losses from the thin edges would usually be negligible. However, this is no longer true in either the normal or superconducting states for highly anisotropic HTC superconductors, where ρ_c/ρ_{ab} in the normal state can typically be as large as 10^5 for $Bi_2Sr_2CaCu_2O_{8+\delta}$ (2212-BSCCO) (Refs. 14 and 15). The normal-state skin depth $\delta_n = (2\rho/\mu_0\omega)^{1/2}$ can therefore be ~ 300 times larger for field penetration through the thin edges (involving current flow in the c direction) than across the major flat faces. Microwave losses from the edges relative to the faces are therefore increased correspondingly. Furthermore, for 2212-BSCCO ρ_c is typically in the range 1–10 Ω cm (Refs. 14 and 15) giving a normal-state skin depth at 10 GHz of $\delta_c \sim 0.5$ to 1.6 mm, which is of the same order as the size of single crystals used in such measurements. Size effects must then be taken properly into

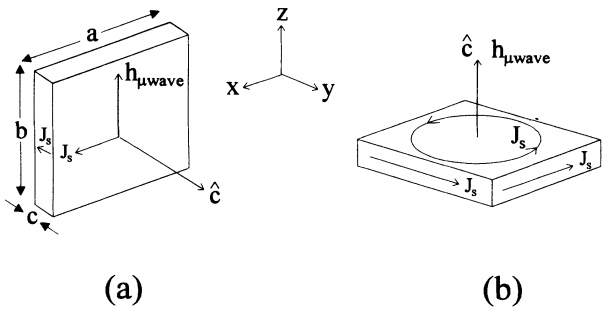

FIG. 1. (a) A thin platelet crystal in the parallel microwave field configuration. The dimensions a, b, and c have been chosen to emphasize the relevance to layered cuprate HTC crystals, where platelet crystals grow with the major faces parallel to the CuO ab planes and c is the thickness of the crystal platelet in the crystallographic c direction, and (b), the perpendicular field configuration, with induced currents confined to the ab planes.

account as derived in this paper. In this configuration, we show that losses from microwave field penetration through the edge surfaces can easily exceed those across the major faces and can rarely be ignored.

Similar complications arise in the superconducting state, since the penetration depth for shielding currents in the c direction is considerably larger than for currents parallel to the faces. For highly anisotropic high-T_c superconductors, such as 2212-BSCCO, $\lambda_{ab}/\lambda_c=\xi_c/\xi_{ab}$, with values typically exceeding 100.[16] The microwave field therefore penetrates ~ 100 times a larger distance through the edge faces than across the principal faces.

In the second experimental configuration of interest, Fig. 1(b) the crystal is aligned with its major flat faces perpendicular to the oscillating microwave field. Measurements are often made in this configuration because the induced microwave currents are confined to the ab planes, so that crystal anisotropy is no longer a problem. However, because of the large demagnetizing factors involved, the induced surface currents are strongly concentrated towards the outer perimeter of the sample and on the thin edge faces. Any imperfections close to the edges of the crystal are therefore likely to result in additional losses associated with weak-link behavior and the resulting degradation of superconducting properties.

II. MICROWAVE ABSORPTION IN THE PARALLEL FIELD CONFIGURATION

A. Normal-state response

We first consider microwave penetration and losses in a resistive platelet crystal with flat faces parallel to the oscillating microwave field $h_{\mu wave}$, as illustrated in Fig. 1(a), which also defines the axes and sample dimensions. The z-dimension length is assumed to be much greater than the thickness so that demagnetizing fields can be ignored; we only need to consider losses per unit length in the z direction.

It is instructive first to derive the electromagnetic response for step and δ-function changes in the external h field. These results can then be used to evaluate the response to a sinusoidal field variation considered as a sequence of δ functions. Such an approach assumes a nonhysteretic, linear electromagnetic response.

Immediately following the removal of a static external field h, the field drops to zero outside the sample but is unchanged within. At $t=0$, the initial field across the area of the rectangular platelet crystal can therefore be written as a double Fourier series

$$h(x,y,0)=h\frac{16}{\pi^2}\sum_{n,m}\frac{1}{nm}\sin\left[\frac{n\pi x}{a}\right]\sin\left[\frac{m\pi y}{c}\right], \tag{1}$$

where n and m are positive odd integers.

The subsequent diffusion of flux out of the platelet is governed by the magnetic diffusion equation. For an anisotropic conductor, Maxwell's equations result in the following anisotropic diffusion equation:

$$\rho_c\frac{\partial^2 h}{\partial x^2}+\rho_a\frac{\partial^2 h}{\partial y^2}=\mu_0\frac{\partial h}{\partial t}, \tag{2}$$

where ρ_a and ρ_c are the resistivities in the ab plane (anisotropy in the ab plane is ignored) and the c direction. Following removal of the external field, the time evolution of the internal field can be written as

$$h(x,y,t)=h\frac{16}{\pi^2}\sum_{nm}\frac{1}{nm}\sin\left[\frac{n\pi x}{a}\right]\sin\left[\frac{m\pi y}{c}\right]e^{-\Lambda_{nm}t}, \tag{3}$$

where

$$\Lambda_{nm}=\frac{\rho_c}{\mu_0}\left[\frac{n\pi}{a}\right]^2+\frac{\rho_a}{\mu_0}\left[\frac{m\pi}{c}\right]^2. \tag{4}$$

Λ_{nm}^{-1} is the time constant for exponential decay of the (n,m) eigenmode solution. At long times the behavior will therefore be dominated by the (1,1) mode. When $(a/c)^2(\rho_c/\rho_a)>1$, the field decays largely through the thin edges of the platelet; when less than unity, it escapes through the major faces. For BSCCO, with an anisotropy in resistance of typically 10^5, flux will escape largely through the thin edges of the crystal, unless the dimensions across the face exceed the thickness by ~ 300. A typical 1-mm platelet crystal would therefore have to be much thinner than 3 μm for edge effects to be ignored, which is seldom satisfied. Note that in the limit of infinite resistance (insulating) in the c direction, the flux motion would be entirely parallel to the ab planes.

To derive the ac response, consider the sinusoidal variation of the microwave magnetic field $he^{i\omega t}$ as a sum of individual δ functions of amplitude $he^{i\omega t'}dt'$ at time t', such that

$$he^{i\omega t}=\int\delta(t-t')he^{i\omega t'}dt'. \tag{5}$$

The overall response at time t is then the sum of the responses from the individual δ functions at times $t'<t$. From Eq. (3), it is easy to show that the response to a unit δ function in field is then given by

$$h(x,y,t)=h\frac{16}{\pi^2}\sum_{nm}\frac{\Lambda_{nm}}{nm}\sin\left[\frac{n\pi x}{a}\right]\sin\left[\frac{m\pi y}{c}\right]e^{-\Lambda_{nm}t}. \tag{6}$$

The time development of the field inside the superconductor in response to an external field varying as $he^{i\omega t}$ is therefore given by

$$H(x,y,t)=h\frac{16}{\pi^2}\int_{-\infty}^{t}\sum_{n,m}\frac{\Lambda_{nm}}{nm}\sin\left[\frac{n\pi x}{a}\right]\sin\left[\frac{m\pi y}{c}\right]\times e^{-\Lambda_{nm}(t-t')}e^{i\omega t'}dt', \tag{7}$$

$$=h\frac{16}{\pi^2}\sum_{nm}\frac{1}{nm}\sin\left[\frac{n\pi x}{a}\right]\sin\left[\frac{m\pi y}{c}\right]\times\frac{\Lambda_{nm}}{\Lambda_{nm}+i\omega}e^{i\omega t}. \tag{8}$$

We evaluate the complex power $P(\omega)$ flowing into the platelet from the time-averaged Poynting vector $\mathbf{E}\times\mathbf{h}^*/2$, where the line integral of E around the perimeter of the platelet normal to the microwave field is given by

$$\oint E\cdot dl=i\omega\mu_0\int H(x,y)dx\,dy$$

$$=i\omega ac\mu_0 h\frac{64}{\pi^4}\sum_{nm}\frac{1}{n^2m^2}\frac{\Lambda_{nm}}{\Lambda_{nm}+i\omega}e^{i\omega t}. \tag{9}$$

The power per unit length along the z direction flowing into the platelet can therefore be written as

$$P(\omega)=\frac{1}{2}he^{-i\omega t}\oint E\cdot dl$$

$$=\frac{i\omega\mu_0h^2ac}{2}\frac{64}{\pi^4}\sum_{nm}\frac{1}{n^2m^2}\frac{\Lambda_{nm}}{\Lambda_{nm}+i\omega}. \tag{10}$$

For an insulator, $\Lambda_{nm}\to\infty$, so that the power flowing into such a crystal, $P_0(\omega)=i\omega\mu_0h^2ac/2$, is simply the (reactive) energy flowing into the equivalent free-space volume per second per unit length, where we have made use of the identity $\sum_{n\text{-odd}}(1/n^2)=\pi^2/8$.

For the more general case of finite conductivities, it is instructive to express the power flowing into the crystal as an effective permeability $\mu(\omega)$, such that $P(\omega)=\frac{1}{2}i\omega\mu(\omega)\mu_0h^2$ per unit volume, where

$$\mu(\omega)=\frac{64}{\pi^4}\sum_{nm}\frac{1}{n^2m^2}\frac{\Lambda_{nm}}{\Lambda_{nm}+i\omega}, \tag{11}$$

so that

$$\mathrm{Re}(P(\omega))=-\tfrac{1}{2}\omega\mu_0h^2\mathrm{Im}(\mu(\omega))$$

and

$$\mathrm{Im}(P(\omega))=\tfrac{1}{2}\omega\mu_0h^2\mathrm{Re}(\mu(\omega)).$$

Λ_{nm} can be expressed in terms of the normal-state skin depths in the a and c directions, δ_a and δ_c, such that

$$\Lambda_{nm}=\frac{\omega\pi^2}{2}\left[\frac{n^2}{(a/\delta_a)^2}+\frac{m^2}{(c/\delta_c)^2}\right], \tag{12}$$

where $\delta_a=\sqrt{2\rho_c/\omega\mu_0}$ and $\delta_c=\sqrt{2\rho_a/\omega\mu_0}$.

The microwave response is therefore determined by the frequency and Λ_{nm} values, which in turn depend on sample dimensions and anisotropic resistivities. It is straightforward to show that the complex microwave power absorbed is identical to the power absorbed in an isotropic sample of the same volume with resistivity $(\rho_a\rho_b)^{1/2}$ but with linear dimensions scaled as $a'=a(\rho_a/\rho_c)^{1/4}$ and $c'=c(\rho_c/\rho_a)^{1/4}$. The large anisotropy of the BSCCO and Tl-Ba-Sr-Cu-O superconductors results in microwave losses per unit area from the edges of platelet crystals being increased relative to the flat faces by a factor $(\rho/\rho_a)^{1/2}$, which typically exceeds a factor >100. Moreover, the poor conductivity in the c direction results in a very long microwave penetration depth parallel to the crystal surfaces, which can easily exceed typical sample dimensions, so that the crystal size effects described by Eq. (11) must be considered.

Before considering Eq. (11) in its most general form, we first consider the microwave power flowing into a thin platelet crystal ignoring any penetration through the edges, as would occur for $\rho_c=0$, when Λ_{nm} is a function of m only. The double summation then reduces to

$$P_a(\omega)=\frac{i\omega\mu_0h^2ac}{2}\frac{8}{\pi^2}\sum_{m}\frac{1}{m^2}\frac{\Lambda_m}{\Lambda_m+i\omega}, \tag{13}$$

where $\Lambda_m=(\omega/2)(\pi m\delta_a/c)^2$. In the Appendix we show that Eq. (13) can be evaluated in analytic form to give $P_a(\omega)=1/2Z_ah^2$ per unit area of the flat faces, where Z_a is the surface impedance of the finite thickness thin slab specimen given by

$$Z_a=iZ_0\tan(kc/2), \tag{14}$$

with $Z_0=\sqrt{i\omega\mu_0\rho_a}$ and $k=(1-i)/\delta_c=\sqrt{\omega\mu_0/i\rho_a}$. This result could, of course, be derived more straightforwardly from the one-dimensional solutions of the diffusion equation subject to the appropriate boundary conditions at the surface.[17]

In Fig. 2 we have plotted the real and imaginary component of $\mu(\omega)$, the complex power flowing into the crystal relative to that flowing into the equivalent free-space volume as a function of $\omega\mu_0c^2/\rho_a=2(c/\delta_c)^2$. On increasing frequency the absolute losses initially increase as $\mu_0^2\omega^2c^3/24\rho_a$ per unit length parallel to the field reaching a peak value of 0.417 of the free-space power penetration, $i\omega\mu_0h^2/2$ per unit volume, when $c/\delta_c\sim2$ as expected. Well above the maximum, the real and imaginary components of the complex surface impedance approach the same values with $R_s=X_s=\sqrt{\mu_0\rho_a\omega/2}=\rho_a/\delta_c$, which is the familiar skin-depth result.

If the sample is a thin platelet of finite area, the properties are affected by microwave field penetration through the edge faces in addition to that across the major flat faces. This does not necessarily lead to an increase in absorbed power, because field penetration at the edges reduces the field gradients and currents flowing parallel

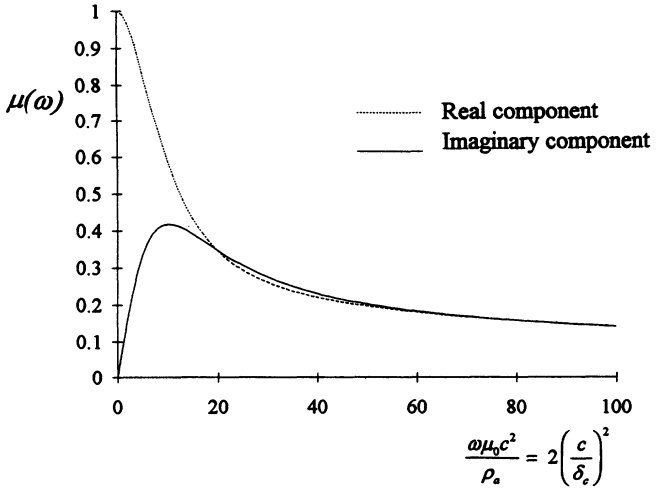

FIG. 2. Electromagnetic energy flowing into a conducting plate of thickness c as a function of $\omega\mu_0 c^2/\rho_a = 2(c/\delta_c)^2$, normalized to the energy flowing into the same free-space volume.

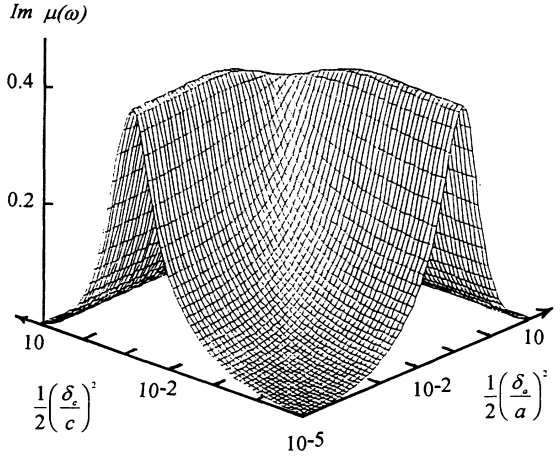

FIG. 3. Two-dimensional plot of the imaginary component of $\mu(\omega)$ for a rectangular rod of cross section $a \times c$ for electromagnetic fields parallel to its length as a function of $\rho_c/\omega\mu_0 a^2$ and $\rho_a/\omega\mu_0 c^2$.

to the major faces, hence reducing microwave losses towards the edges of the major flat surfaces. In general, the losses determined by Eq. (11) depend in a rather complicated way on the frequency, the anisotropic resistivities, and the sample dimensions.

The convergence of the double summation in Eq. (11) is extremely slow, particularly for the reactive component. It is therefore convenient to replace one of the summations by an analytic expression similar to that obtained for the infinite slab geometry, as described in the Appendix. The effective permeability of the platelet crystal can then be expressed as

$$\mu(\omega) = \frac{16}{\pi^3} \sum_{nm} \frac{1}{n^2} \left[\frac{\tan(\pi\alpha_n/2)}{\alpha_n} + \frac{\tan(\pi\gamma m/2)}{\gamma_m} \right], \quad (15)$$

where

$$\alpha_m^2 = -i\left\{ \omega \frac{\mu_0}{\rho_c} \left[\frac{a}{\pi} \right]^2 - i \frac{\rho_a a^2}{\rho_c c^2} m^2 \right\}$$

and

$$\gamma_n^2 = -i\left\{ \omega \frac{\mu_0}{\rho_a} \left[\frac{c}{\pi} \right]^2 - i \frac{\rho_c c^2}{\rho_a c^2} n^2 \right\}.$$

The above expression converges relatively rapidly and can readily be evaluated using standard computer routines.

Both terms in Eq. (15) depend on the ratio of the appropriate skin depth to the sample dimension, as in the infinite thin slab geometry, but in addition also depend on the ratio

$$\frac{\rho_a a^2}{\rho_c c^2} = \frac{(a/\delta_a)^2}{(c/\delta_c)^2}.$$

Microwave field penetration through both the flat faces and the side edges reduces the size of the loss peak, as indicated in Fig. 3, where we show a two-dimensional plot of the imaginary (loss) component of $\mu(\omega)$ as a function of $\rho_c/\omega\mu_0 a^2$ and $\rho_a/\omega\mu_0 c^2$. This diagram shows that the affect of considering microwave losses from all four faces parallel to the field is always to reduce the peak in microwave loss relative to that calculated across any two parallel faces alone. By symmetry, the minimum value of the loss peak occurs when $\rho_c c^2/\rho_a a^2 = 1$, where

$$\mu_{\text{symmetric}} = \frac{32}{\pi^3} \sum_n \frac{1}{n^2} \frac{\tan(\pi\alpha/2)}{\alpha}, \quad (16)$$

which is equivalent to the result for an isotropic square rod. This function is plotted in Fig. 4 as a function of $2(a/\delta_a)^2 = 2(c/\delta_c)^2$, where comparison is made with

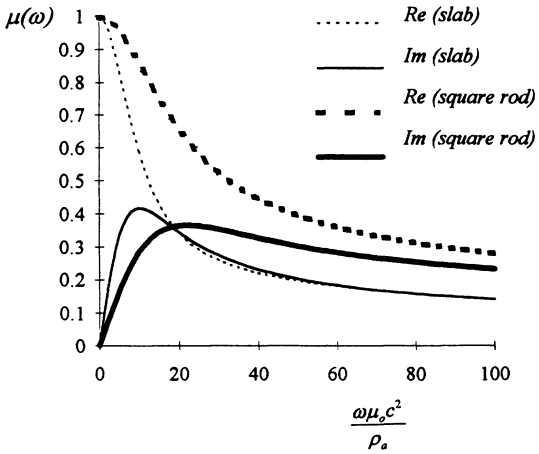

FIG. 4. The dependence of the complex magnetic permeability $\mu_{\text{symmetric}}$ of a rectangular rod with cross-section dimensions such that $a^2/\rho_a = b^2/\rho_c$ (equivalent to the isotropic square cross-section rod problem) compared with μ evaluated for a finite thickness slab, both plotted as a function of $\omega\mu_0 c^2/\rho_a$. The solid lines represent the resistive components and the dashed lines the reactive.

$\mu(\omega)$ evaluated for the thin slab geometry. These calculations place absolute limits on the magnitude of the loss peak observed in any ac or microwave absorption measurement of between 0.366 and 0.417 of the power flowing into the equivalent free-space volume. We note that, for purely resistive microwave losses, changes in sample anisotropy with temperature or field can only vary the size of the loss peak by 13% below its maximum value.

In a cavity perturbation experiment the (complex) fractional shift in frequency introduced by a small platelet can be written as

$$\frac{\Delta f}{f}=-\frac{1}{2}(1-\mu)\frac{h_s^2\times\text{sample volume}}{\int h^2_{\text{cavity}}d^3r}\ , \tag{17}$$

where h_s is the microwave field at the sample position and h_{cavity} is the cavity field. Provided the geometric factor associated with the field distribution within the cavity is known, measured changes in resonant frequency and Q factor can be used to derive absolute values for the changes in the real and imaginary components of $\mu(\omega)$.

B. Superconducting state

In the Meissner state, the electromagnetic field penetrates a distance $\lambda(T)$ into the sample. We confine our discussion to situations where this length is very much less than the sample dimensions. The power absorption $P(\omega)$ per unit length in the field direction of a platelet crystal is then simply the sum of the power absorbed on the major faces and the edges, given by

$$P(\omega)=(Z_a a+Z_c c)h^2\ . \tag{18}$$

We assume a two-fluid model for the anisotropic superconductor such that

$$Z_{a,c}=i\omega\mu_0\lambda_{a,c}+(1/2)\omega^2\mu_0^2\lambda_{a,c}^3\sigma_{a,c}\ , \tag{19}$$

where the subscripts refer to the appropriate crystallographic directions, and the penetration depth and the quasiparticle conductivity in both directions will depend on temperature. The reactive contribution from the flat faces relative to the edges is therefore $a\lambda_a/c\lambda_c$, while the ratio of the resistive components is $a\lambda_a^3\sigma_a/c\lambda_c^3\sigma_c$. A possible method to distinguish between the contributions from the flat faces and the edges would be to use a rectangular rather than a square platelet and to perform measurements first with the long edge and then with the short edge parallel to the field, which would allow an independent evaluation of all four unknowns provided the sample properties are uniform.

In a high-T_c superconductor an applied magnetic field perpendicular to the ab planes introduces flux lines or two-dimensional pancakes, which at low temperatures are forced to oscillate about their pinning sites by the induced microwave currents. This leads to an increased penetration depth λ_C, the Campbell penetration depth,[18] related to the strength and spatial variation of the pinning potential, and to additional damping from viscous flux flow.[19,20] At sufficiently high temperature the flux lines are thermally excited out of their pinning sites and are subject only to resistive damping. If this damping is described by a flux-flow resistivity of the form proposed by Bardeen-Stephen,[21] with $\rho\sim(B/B_{c2})\rho_n$, the effective penetration depth will be $\sim(B/B_{c2})^{1/2}\delta_n$, which approaches the normal-state value at $T_{c2}(B)$.

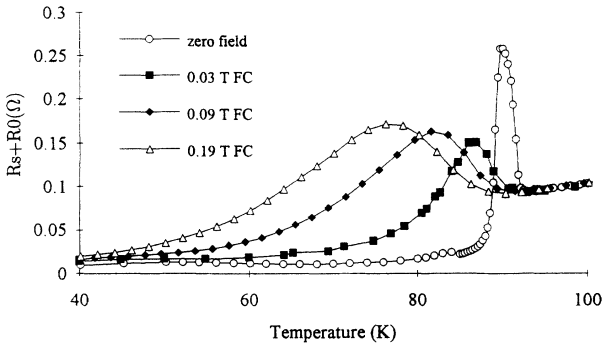

FIG. 5. R_s as a function of temperature for a thin platelet 2212-BSCCO single crystal with rf field parallel to the flat faces and external dc magnetic fields parallel to c.

While measurements on YBCO thin films[23] and single crystals are consistent with an approximate $B^{1/2}$ dependence, this is not observed in 2212-BSCCO single crystals.[22] In 2212-BSCCO an anomalous peak in the loss has even been observed in one crystal, which moves to lower temperatures on increasing field,[23] as illustrated in Fig. 5. We account for this behavior by assuming that in the normal state the microwave penetration depth through the thin edges of the crystal is larger than the lateral dimensions of the crystal (~2 mm). As the sample is cooled through T_c, the resistance in the c direction eventually decreases until the penetration depth becomes comparable with the lateral dimensions of the major faces of the crystal resulting in the expected peak in microwave loss, the loss going to zero at lower temperatures as the resistance decreases further. As expected the peak moves to lower temperatures in the presence of a magnetic field because of the B dependence of the c-direction resistivity.[14,15] If a simple resistive model for the conductivity along the c direction is assumed, with microwave losses entirely determined by penetration through the edges, an estimate of $\rho_c(T,B)$ can be made.[24]

In practice, as we have shown above, the size of the loss peak will depend on the resistivities parallel to the ab planes and c directions, but assuming resistive losses only, the peak height can only vary by 13%. A resistive model alone therefore cannot account for the much larger variations in peak height observed in Fig. 5. The larger variation in height of the loss peak can, however, be modeled by including a reactive term in the conductivity along the c axis, as would be expected if we model the conductivity in terms of parallel arrays of weakly coupled resistively shunted Josephson junctions, as proposed to describe the $V(I)$ characteristics and coherent microwave radiation for small single crystals.[24]

III. PERPENDICULAR FIELD CONFIGURATION

A. Normal state

Microwave cavity perturbation measurements are frequently made with platelet crystals oriented perpendicu-

lar to the microwave h field, as illustrated in Fig. 1(b). The induced microwave currents then flow parallel to the ab plane so that crystalline anisotropy is no longer a problem.

At sufficiently high frequencies, the normal-state microwave penetration depth δ_n will be much less than any crystal dimension, so that the field distribution over the surface can be approximated by assuming near perfect diamagnetic behavior. An estimate of the surface fields for a flat platelet slab can then be made from the known solutions for an oblate ellipsoid of revolution[25] of the same maximal dimensions, as illustrated in Fig. 6. In a recent paper, Parvin *et al.*[26] have derived the general result for the ac response of a conducting oblate spheroid over the whole frequency range, from low frequencies giving near complete flux penetration to the high-frequency situation considered here.

At high frequencies, the problem is reduced to considering the microwave losses $\frac{1}{2}h_s^2 Z_s$ per unit area of the surface, where h_s is the component of the microwave field parallel to the surface. This can be evaluated by noting that the h field inside a uniformly magnetized ellipsoid of revolution is uniform and is equal to the external field h_0 at the perimeter. For a diamagnetic ellipsoid of revolution with $c/a \ll 1$, $h_0 = h_{\text{applied}}/(1-D)$, where $D = 1-(\pi/2)(c/a)$,[25] so that $h_0 = (2/m\pi)h_{\text{applied}}$ with $m = c/a$.

Simple geometrical considerations then enable us to express the field parallel to the surface as a function of radial distance as

$$h_s(r) = h_0 \frac{mr}{\sqrt{1-r^2+m^2r^2}} , \tag{20}$$

where $r = x/a$ is the normalized radial distance. The surface field normalized to h_0 is plotted for a few representative m values in Fig. 7. Note the very strong field enhancement within a normalized distance $\sim m^2/2$ from the edge.

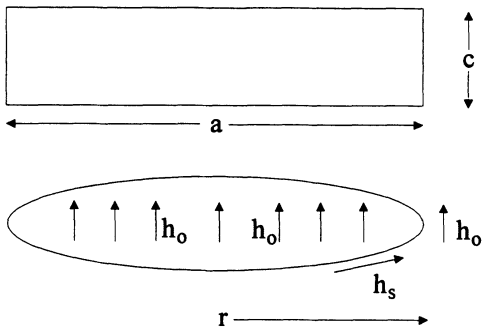

FIG. 6. A flat platelet crystal and the circumscribed ellipsoid of revolution referred to in text. Note that the internal field inside the ellipsoid is uniform and is equal to $h_0 = (2a/\pi c) \times$ the applied microwave field amplitude at a distance from the sample.

The microwave power flowing into the sample is even more peaked towards the outer edges because of the singularity in surface area with respect to r at the perimeter. The microwave power, $\frac{1}{2}h_s^2 Z_s$ per unit area, contributes to an integrated power input $P(r)$ as a function of normalized radial distance given by

$$P(r) = \int_0^r \frac{1}{2} h_s^2 Z_s \, ds \tag{21}$$

so that the normalized integrated power absorption is given by

$$\frac{P(r)}{P(1)} = \int_0^r \frac{mr^3}{\sqrt{1-r^2+m^2r^2}} \frac{dr}{\sqrt{1-r^2}} \Big/ \int_0^1 \frac{mr^3}{\sqrt{1-r^2+m^2r^2}} \frac{dr}{\sqrt{1-r^2}} , \tag{22}$$

which is illustrated in Fig. 8 for the same m values used in Fig. 7. The energy absorption is very strongly peaked within a short distance $\sim m^2 a = c^2/a$ of the outer perimeter. For example, for a crystal with aspect ratio $a/c = 10$, $\sim 50\%$ of the power absorbed is concentrated within 1% of the radial distance from the outer edge of the ellipsoid. Although the exact behavior will clearly be highly shape dependent, we would expect a similar behavior for a flat platelet crystal, with the major power absorption being strongly concentrated towards the outer perimeter edges of the flat crystal faces. There will be a major contribution from the edge faces also. The degree of perfection of such edges may then be more important than the perfection of the major flat area, most of which contributes very little to the microwave power absorption.

B. Superconducting state

In this configuration, the microwave currents and losses will again largely be concentrated very close to the

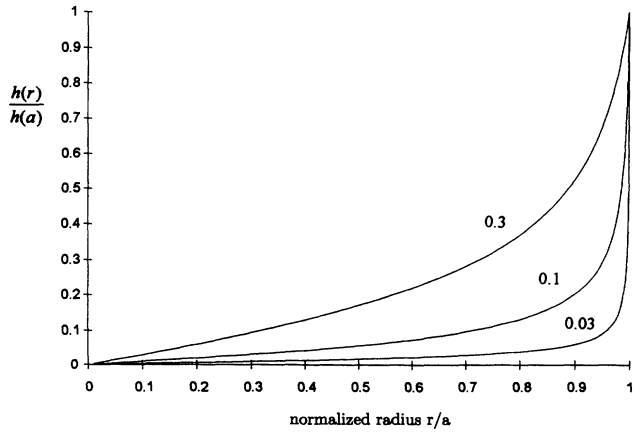

FIG. 7. The field $h_s(r)$ parallel to the surface as a function of normalized radial distance normalized to the field $h_s(1)$ at the edge for representative values of $m = c/a$.

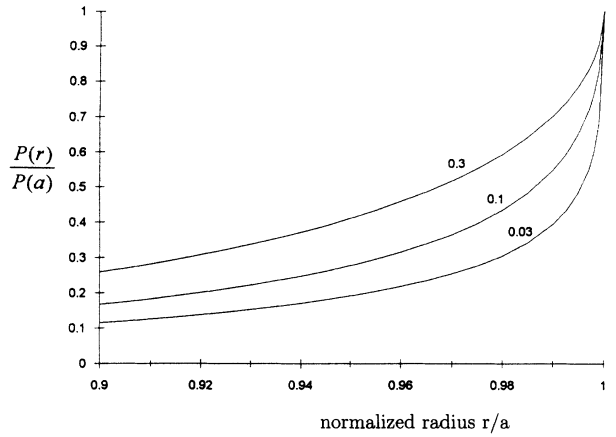

FIG. 8. The normalized power absorbed $P(r)$ within the normalized radial distance r, for representative values of $m=c/a$, illustrating the extremely strong peaking of power absorption towards the perimeter of the sample.

outer perimeter, as remarked above. Flux is effectively excluded over a sphere of radius a, so that the changes in moment on making a transition from the normal to the superconducting state are $\sim 4\pi a^2[\delta_a-\lambda(T)+\Delta l(T)]$, compared with $\sim 2\pi a^2[\delta_a-\lambda(T)+\Delta l(T)c/a]$ for the parallel configuration, where $\Delta l(T)$ is the change in a dimension over the measured temperature range. The sensitivity is therefore not very different for the two configurations. In both cases it may be necessary to make corrections for changes in the magnetization due to thermal expansion, which will be more important for the perpendicular field orientation. These corrections may significantly affect the derived reactive component of the surface impedance. In general the losses in the superconducting state in this configuration depend on geometric factors, which are usually poorly defined. Most authors therefore simply quote measurements in the superconducting state relative to those in the normal state just above the transition, which are assumed to be given by the measured (or assumed) normal-state resistivity.

IV. CONCLUSIONS

In conclusion, we have considered the microwave properties of the anisotropic thin platelet high-T_c crystals oriented with their major flat faces parallel or perpendicular to the oscillating h field for both normal and superconducting states.

In the parallel field configuration, the microwave properties in both the normal and superconducting states are strongly influenced by the very large anisotropy of the resistivity parallel and perpendicular to the ab planes. In addition, finite-size effects can lead to an anomalous peak in the absorption below T_c, if the microwave penetration depth in the normal state is larger than the sample dimensions. This accounts, at least qualitatively, for the temperature and field dependence of a peak in the microwave loss below T_c observed in some 2212-BSCCO crystals, though the conducting properties along the c direction must be generalized to include a reactive, supercurrent, component to account for the observed variation in peak height.

In the perpendicular configuration, the large demagnetizing factor causes a large concentration of the microwave field towards the outer perimeter of the crystal. For an oblate ellipsoid of rotation circumscribed by the platelet volume, the microwave losses are concentrated within a distance $\sim c^2/a$ of the perimeter. Although this concentration of microwave field towards the outer edges of a crystal will, in practice, be strongly shape dependent, it is always likely to be important in practice. Care must therefore be taken to avoid damage to the outer edges of a crystal, if the microwave measurements are not to be degraded by localized defect structures.

ACKNOWLEDGMENTS

We wish to acknowledge many valuable discussions with Dr. Adrian Porch and Dr. Mike Lancaster and for the support of the SERC in funding this research and to the National Physical Laboratory for supporting a CASE studentship for one of us (N.J.E.).

APPENDIX

To evaluate Eq. (13) for the complex power per unit length flowing into a finite thickness slab, we first rewrite $P_a(\omega)$ in the form

$$P_a(\omega)=\frac{i\omega\mu_0 h^2 ac}{2}\mu(\omega)\ , \tag{A1}$$

where the effective permeability may be written as

$$\mu(\omega)=\frac{8}{\pi^2}\sum_m \frac{1}{m^2}\frac{\Lambda_m}{\Lambda_m+i\omega}\ , \tag{A2}$$

and $\Lambda_m=\rho/\mu_0(\pi/c)^2m^2=\alpha m^2$, where m is an odd integer. Equation (A2) can then be rewritten as

$$\mu(\omega)=\frac{8}{\pi^2}\sum_{m\text{-odd}}\frac{1}{m^2+i\omega/\alpha}=\frac{8}{\pi^2}\sum_{m\text{-odd}}\frac{1}{m^2-\beta^2}\ , \tag{A3}$$

where $\beta^2=\omega/i\alpha$.

To evaluate this series, we consider the contour integral $\oint[\tan(z\pi/2)/(z^2-\beta^2)]dz$ around a contour along the imaginary axis and a semicircle at infinity enclosing the poles $2/\pi(m-z)$ of the tan function when $z=m$ (positive odd integers) and the pole at $+\beta$. The integrals along the imaginary axis and at infinity are zero. We may therefore write

$$\frac{2}{\pi}\sum_{m\text{ odd}}\frac{1}{m^2-\beta^2}=\frac{\tan(\pi\beta/2)}{2\beta}\ , \tag{A4}$$

so that

$$\mu(\omega)=\frac{\tan(\pi\beta/2)}{\pi\beta/2}\ . \tag{A5}$$

The surface resistance Z_S for the slab geometry is given by equating the energies per unit area flowing into the two surfaces $Z_s h^2=i\omega\mu\mu_0 a h^2/2$, so that

$$Z_s = ia\omega\mu_0 \frac{\tan(\pi\beta/2)}{\pi\beta} = iZ_0 \tan(kc/2) , \quad \text{(A6)}$$

where $Z_0 = \sqrt{i\omega\mu_0\rho}$ and $k = \sqrt{\omega\mu_0/i\rho}$, which is the required result.

We now consider the more general case of the platelet crystal with rectangular cross section, where $\mu(\omega)$ may be written as

$$\mu(\omega) = \frac{64}{\pi^4} \sum_{nm} \frac{\Lambda_{nm}}{n^2 m^2} \frac{1}{\Lambda_{nm} + i\omega} , \quad \text{(A7)}$$

with

$$\Lambda_{nm} = \frac{\rho_c}{\mu_0} \left[\frac{n\pi}{a} \right]^2 + \frac{\rho_a}{\mu_0} \left[\frac{m\pi}{c} \right]^2 . \quad \text{(A8)}$$

We may write Eq. (A7) as

$$\mu(\omega) = \frac{64}{\pi^4} \sum_{nm} \left[\frac{1}{m^2} \frac{1}{n^2 - \alpha_m^2} + \frac{1}{n^2} \frac{1}{m^2 - \gamma_n^2} \right] , \quad \text{(A9)}$$

where

$$\alpha_m^2 = -i \left\{ \omega \frac{\mu_0}{\rho_c} \left[\frac{a}{\pi} \right]^2 - i \frac{\rho_a a^2}{\rho_c c^2} m^2 \right\}$$

and

$$\gamma_n^2 = -i \left\{ \omega \frac{\mu_0}{\rho_a} \left[\frac{c}{\pi} \right]^2 - i \frac{\rho_c c^2}{\rho_a c^2} n^2 \right\} .$$

Each term can now be summed separately over one of the integers to give

$$\mu(\omega) = \frac{16}{\pi^3} \sum_{n} \frac{1}{n^2} \left[\frac{\tan(\pi\alpha_n/2)}{\alpha_n} + \frac{\tan(\pi\gamma_n/2)}{\gamma_n} \right] , \quad \text{(A10)}$$

which is now a rapidly convergent series of the single odd integer n.

[1] A. Porch and J. R. Waldram, in *Concise Encyclopedia of Magnetic and Superconducting Materials,* edited by J. Evetts (Pergamon, New York, 1992), p. 183.

[2] A. M. Portis, in *Earlier and Recent Aspects of Superconductivity,* edited by J. G. Bednorz and K. A. Muller, Springer Series in Solid State Sciences, Vol. 90 (Springer-Verlag, Berlin, 1990), p. 278.

[3] H. Piel and G. Muller, IEEE Trans. Magn. **27**, 85 (1991).

[4] J. F. Annet, N. D. Goldenfeld, and S. R. Renn, Phys. Rev. B **43**, 2778 (1991).

[5] J. M. Pond, K. R. Carroll, J. S. Horowitz, D. B. Chrisey, M. S. Osofsky, and V. C. Cestone, Appl. Phys. Lett. **59**, 3033 (1991).

[6] S. M. Anlage and D-H. Wu, J. Supercond. **5**, 395 (1992).

[7] W. N. Hardy, D. A. Bonn, D. C. Morgan, R. Liang, and K. Zhang, Phys. Rev. Lett. **70**, 3999 (1993).

[8] J. F. Annet, N. D. Goldenfeld, and S. R. Renn, in *Physical Properties of High-Temperature Superconductors II,* edited by D. M. Ginsberg (World Scientific, New Jersey, 1990).

[9] P. J. Hirschfeld and N. Goldenfeld, Phys. Rev. B **48**, 4219 (1993).

[10] D. A. Bonn, R. Liang, T. M. Riesman, D. J. Bear, D. C. Morgan, K. Zhang, P. Dosanjih, T. L. Duty, A. MacFarlane, G. D. Morris, J. H. Brewer, W. N. Hardy, C. Kallin, and A. J. Berlinsky, Phys. Rev. B **47**, 11 314 (1993).

[11] A. Porch, M. J. Lancaster, and R. G. Humphreys, Physica B **194-196**, 1605 (1994).

[12] J. Rossat-Mignod, L. P. Regnaults, C. Vettier, P. Bourges, P. Burlet, J. Bossy, J. Y. Henry, and G. Lapertov, Physica C **185-189**, 86 (1991).

[13] S. E. Barrett, J. A. Martindale, D. J. Durand, C. H. Pennington, C. P. Slichter, T. A. Friedmann, J. P. Rice, and D. M. Ginsberg, Phys. Rev. Lett. **66**, 108 (1991).

[14] S. Martin, A. T. Fiory, R. M. Fleming, L. F. Schneemeyer, and J. V. Waszczak, Phys. Rev. Lett. **60**, 2194 (1988).

[15] V. R. Busch, G. Ries, H. Werthner, G. Kreiselmeyer, and G. Saemann-Ischnko, Phys. Rev. Lett. **69**, 522 (1992).

[16] J. C. Martinez, S. H. Brongersma, A. Koshalev, B. Ivlev, P. H. Kes, R. P. Briessen, D. G. de Groot, Z. Tarnavski, and A. A. Menovsky, Phys. Rev. Lett. **69**, 2276 (1992).

[17] A. Porch, J. R. Waldram, and L. F. Cohen, J. Phys. F **18**, 1547 (1988).

[18] A. M. Campbell, J. Phys. C **4**, 3186 (1971).

[19] M. W. Coffey and J. R. Clem, Physica C **185-189**, 1915 (1991).

[20] E. H. Brandt, Phys. Rev. Lett. **67**, 2219 (1991).

[21] J. Bardeen and M. H. Stephen, Phys. Rev. A **140**, 1197 (1965).

[22] J. Owliaei, S. Sridhar, and J. Talvacchio, Phys. Rev. Lett. **69**, 3366 (1992).

[23] N. Exon, M. Lancaster, A. Porch, G. Yang, and C. E. Gough, IEEE Trans Appl. Supercond. **3**, 1442 (1993).

[24] R. Kleiner, F. Steinmeyer, G. Kunkel, and P. Muller, Phys. Rev. Lett. **68**, 2394 (1992).

[25] E. C. Stoner, Philos. Mag. **36**, 803 (1945).

[26] E. M. Parvin, A. Singfield, W. F. Vinen, and G. F. Cox, Supercond. Sci. Technol. **6**, 525 (1993).